



## Optimization of 4,6-bis-anilino-1*H*-pyrrolo[2,3-*d*]pyrimidine IGF-1R tyrosine kinase inhibitors towards JNK selectivity

Stanley D. Chamberlain<sup>a</sup>, Anikó M. Redman<sup>a</sup>, Joseph W. Wilson<sup>a</sup>, Felix Deanda<sup>b</sup>, J. Brad Shotwell<sup>a</sup>, Roseanne Gerding<sup>a</sup>, Huangshu Lei<sup>a</sup>, Bin Yang<sup>a</sup>, Kirk L. Stevens<sup>a</sup>, Anne M. Hassell<sup>a</sup>, Lisa M. Shewchuk<sup>b</sup>, M. Anthony Leesnitzer<sup>a</sup>, Jeffery L. Smith<sup>a</sup>, Peter Sabbatini<sup>c</sup>, Charity Atkins<sup>c</sup>, Arthur Groy<sup>c</sup>, Jason L. Rowand<sup>c</sup>, Rakesh Kumar<sup>c</sup>, Robert A. Mook Jr.<sup>a</sup>, Ganesh Moorthy<sup>c</sup>, Samarjit Patnaik<sup>a,\*</sup>

<sup>a</sup> GlaxoSmithKline, Oncology R&D, 5 Moore Drive, Research Triangle Park, NC 27709, USA

<sup>b</sup> GlaxoSmithKline, Computational and Structural Chemistry, 5 Moore Drive, Research Triangle Park, NC 27709, USA

<sup>c</sup> GlaxoSmithKline, Oncology R&D, 1250 S. Collegeville Road, Collegeville, PA 19426, USA

### ARTICLE INFO

#### Article history:

Received 8 October 2008

Revised 19 November 2008

Accepted 20 November 2008

Available online 24 November 2008

#### Keywords:

IGF-1R

IGF-1R

JNK

Pyrrolopyrimidine

### ABSTRACT

The SAR of C5' functional groups with terminal basic amines at the C6 aniline of 4,6-bis-anilino-1*H*-pyrrolo[2,3-*d*]pyrimidines is reported. Examples demonstrate potent inhibition of IGF-1R with 1000-fold selectivity over JNK1 and 3 in enzymatic assays.

© 2008 Elsevier Ltd. All rights reserved.

Aberrant signaling through the insulin-like growth factor-1 receptor (IGF-1R) has been implicated as a key process in tumor progression and resistance to cancer therapy.<sup>1</sup> Several small molecular inhibitors which inhibit this pathway via binding to the intracellular kinase domain have been reported.<sup>2</sup> In the preceding communication, we reported a series of novel 4,6-bis-anilino-1*H*-pyrrolo[2,3-*d*]pyrimidines with a variety of 4' cyclic tertiary amines at the C6 aniline as potent inhibitors of the IGF-1R tyrosine kinase.<sup>3</sup> A C4' isopropyl piperazine **1** was particularly noteworthy with an optimal potency and pharmacokinetic profile.<sup>4</sup> In a preliminary panel of 57 kinases **1** showed IC<sub>50</sub> values  $\geq 100$  nM ( $\geq 50$ -fold selectivity) against 52 kinases, with IC<sub>50</sub> measurements for ALK, IGF-1R, IR, JNK1, and JNK3 at 0.5 nM, 2.0 nM, 1.6 nM, 13 nM, and 100 nM, respectively. When the isopropyl piperazine substituent was moved to the C5' position (**2**) the IGF-1R potency was retained (Table 1). Interestingly, the presence of an additional C4' methyl substituent (**3**) dropped the IGF-1R enzyme potency by 10-fold. More importantly, the C5' isopropyl piperazine **2** also seemed to impart superior selectivity against JNK1 and 3 over its C4' counterpart **1**.<sup>5</sup>

The Jun N-terminal kinases (JNKs) are mitogen activated protein kinases that play a well established role in immune response. They

are activated by environmental stress and proinflammatory cytokines like tumor necrosis factor- $\alpha$  and interleukin-1.<sup>6</sup> The JNKs modulate the activity of multiple transcription factors which regulate diverse cellular functions such as apoptosis, survival, and protein degradation,<sup>7</sup> and have also been implicated in oncogenic transformation.<sup>8</sup> They are also intimately involved in cross-talk with other signaling networks including the NF- $\kappa$ B pathway.<sup>9</sup> In light of the complicating activities associated with JNK inhibition we felt that the selectivity demonstrated by pyrrolopyrimidines **2** and **3** was preferable in order to understand the phenotypic effects of inhibiting the IGF-1R signaling.

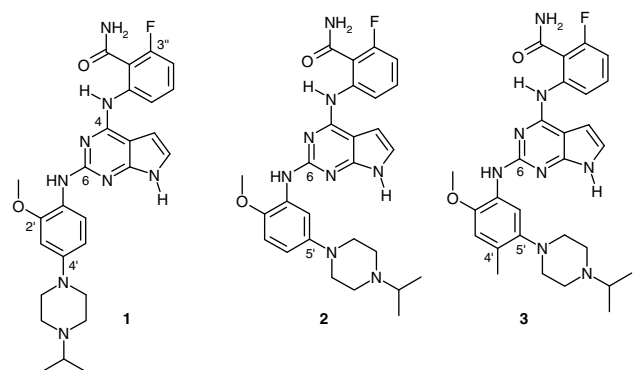
We constructed a docking model of **2** in complex with the IGF-1R kinase domain to probe its binding mode (Fig. 1). As expected, most of the inhibitor was predicted to have similar interactions with the enzyme as **1** except the C5' 4-isopropyl piperazine.<sup>10</sup> The latter lay at the entrance of the ATP-binding site directed towards the  $\alpha$ D helix where it was predicted to participate in an ionic interaction with the carboxylate of Asp1056. This ionic interaction forced the backbone NH of Asp1056 to make unfavorable van der Waals contact with the ethylene portions of the piperazinyl moiety. Additionally, the *N*-isopropyl made contact with the hydroxyl of Ser 1059. Thus, any gain in potency resulting from the ionic interaction might be offset or negated by unfavorable polar-nonpolar interactions. This may explain why **1** and **2** are essentially equipotent on IGF-1R enzyme. A similar docking model of **3** was also

\* Corresponding author. Tel.: +1 919 4836229; fax: +1 919 4836053.

E-mail address: [samarjitpatnaik@gmail.com](mailto:samarjitpatnaik@gmail.com) (S. Patnaik).

**Table 1**

IGF-1R, JNK1, and JNK3 potencies for **1–3** (values represent an average of  $\geq 2$  individual measurements)



Compound	IGF-1R enzyme IC <sub>50</sub> (nM)	JNK1 enzyme IC <sub>50</sub> (nM)	JNK3 enzyme IC <sub>50</sub> (nM)	Phospho IGF-1R cellular IC <sub>50</sub> (nM)
<b>1</b>	2	13	100	117
<b>2</b>	4	3162	5011	201
<b>3</b>	20	3891	6310	270

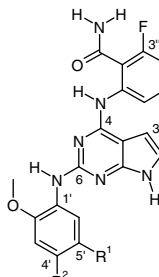
constructed (not shown), yielding a binding mode that was nearly identical to that of **2** with one significant difference. The orientation of the C5' piperazinyl was rotated further out-of-plane with respect to the C6 aniline compared to that of **2**, perhaps to minimize steric clash with the C4' methyl. This change disrupted the ionic interaction between the inhibitor and Asp1056, which was perhaps reflected in its reduced IGF-1R enzyme IC<sub>50</sub> value of 20 nM.

We decided to further evaluate the potential of the unique interaction with Asp1056 by substituting a variety of functional groups at C5' with terminal amines. We were particularly interested in addressing a hypothesis that such substituents might lead to significant reductions in the inhibitory activity against JNK1 and 3 as evidenced by **2** and **3**. We decided, at the outset, to retain the optimal C2'-methoxy aniline at C6 and the C3'-fluoroanthranilamide at C4 to maintain selectivity and pharmacokinetic proper-

ties.<sup>3</sup> Listed in Table 2 are analogs that were synthesized and screened in our study. Notably, all compounds maintained greater than 75-fold selectivity for IGF-1R over JNK1 and 3<sup>11</sup> (not shown in Table 2) except **7**, which still had a better selectivity than **1**. Most analogs with a C4' chloro or methyl substituent (**5**, **7**, **9**) seemed to reduce the IGF-1R cellular activity by 4- to 10-fold compared to their unsubstituted counterparts (**4**, **6**, **8**). However, the C5' *N,N*-dimethylglycinamide containing molecules (**10–13**) displayed an unanticipated IGF-1R activity profile with a toleration of methylation at C4' (**11**). On the other hand, methylation of the amide nitrogen proved deleterious toward cell potency (**12** and **13**), emphasizing that rotational restrictions around the amide bond may interfere with a favorable disposition of the basic amine in the enzyme pocket. Compounds **10** and **11**, which contained the *N,N*-dimethylglycinamide substituent, had the most promising potency and selectivity profiles with >5-fold improvement over the

**Table 2**

IGF-1R enzyme and Delfia, JNK1 results for **4–13** (values represent an average of  $\geq 2$  individual measurements)



Compound	R <sup>1</sup>	R <sup>2</sup>	IGF-1R enzyme IC <sub>50</sub> (nM)	Phospho IGF-1R cellular IC <sub>50</sub> (nM)	JNK1 enzyme IC <sub>50</sub> (nM)
<b>4</b>		H	8	81	631
<b>5</b>		Cl	13	895	1258
<b>6</b>		H	13	212	5011
<b>7</b>		CH <sub>3</sub>	13	840	501
<b>8</b>		H	6	929	1258
<b>9</b>		Cl	25	5366	3981
<b>10</b>		H	1	28	3162
<b>11</b>		CH <sub>3</sub>	0.5	38	1995
<b>12</b>		H	50	377	10,000
<b>13</b>		CH <sub>3</sub>	63	1728	10,000



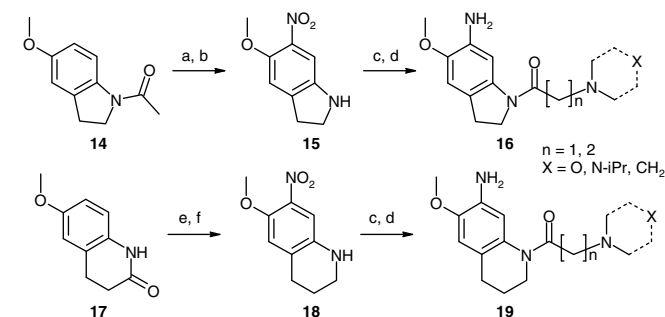
**Figure 1.** Structural model of IGF-1R (carbon atoms in gray) in complex with **2** (carbon atoms in green). The 4-isopropyl piperazine's methyl groups in **2** are overlapped in this pose. Intermolecular H-bond and ionic interactions are highlighted with yellow lines.

IGF-1R cellular potency of **2**. The toleration of the C4' methyl by **11** prompted a further exploration of analogs where the C5' amide nitrogen was constrained back onto C4'. To that end we synthesized indoline and tetrahydroquinoline precursors, as illustrated in Scheme 1, and concentrated on amides with pendant amines to expand on the SAR demonstrated by **10** and **11**.

Regioselective nitration of commercially available **14** with acetic anhydride/nitric acid followed by deacetylation provided multi-gram quantities of **15**. This pivotal intermediate provided an easy access to multiple analogs with the indoline substructure. To that end **15** was acylated with bromoacetyl bromide, and subjected to bromide displacement with various cyclic and acyclic secondary amines. Acylation of **15** with acryloyl chloride followed by amine addition provided the corresponding one carbon homologated analogs. Final reduction of the nitro functionality provided anilines **16** which could be installed into the pyrrolopyrimidine core via  $S_NAr$  chemistry described in detail in a previous communication.<sup>12</sup> Synthesis of the corresponding ring-expanded tetrahydroquinolines started with nitration of lactam **17**.<sup>13</sup> Subsequent borane reduction provided the intermediate tetrahydroquinoline **18** which was derivatized to **19**.

Table 3 lists the biological results from our systematic evaluation of nitrogen substituents in the constrained ring systems. The acetyl group of indoline **20** yielded a modest inhibitor in the IGF-1R cellular mechanistic assay. Although the attachment of a primary amine (**21**) worsened cell activity, the selectivity over JNK1 improved.<sup>11</sup> However, single digit nanomolar IGF-1R potencies and three orders of magnitude selectivity over JNK1 were obtained with the methyl amine in **22**, small acyclic secondary amines (**23**, **24**, **26**), and small cyclic amines (**27**, **28**). Reduction in amine basicity lowered either cell potency (**25**) or selectivity (**30**). Compounds with an ethylene between the amide carbonyl and amine (**32–34**), in general, exhibited reduced cellular potency than their non-homologated congeners. Removal of the amide carbonyl from **23** in **35** lowered IGF-1R potency and selectivity against JNK1. The SAR observed in the indoline series was reflected in the tetrahydroquinolines (**36–39**). A simple acetyl on the ring nitrogen (**36**) had modest cell potency which was rescued by the dimethylated amine or piperidinyl analogs **37** and **38**, respectively. These compounds had the most favorable activity and selectivity parameters. The presence of an extra carbon atom between the amide and amine in **39** reduced IGF-1R cell potency. Thus a variety of indolines (**22–24**, **26–28**) and tetrahydroquinolines (**37**, **38**) had a similar potency and selectivity profile as the unconstrained analogs **10** and **11**.

A better understanding of the SAR depicted in Table 3 was achieved when a co-crystal structure of **40** (Fig. 2A, structure in white) in complex with an Insulin Receptor (IR) mutant (C981S, D1132N) was solved, revealing the inhibitor's binding mode.<sup>14,15</sup>



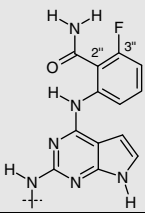
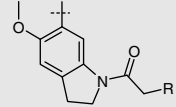
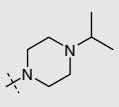
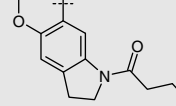
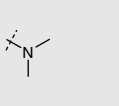
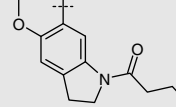
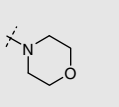
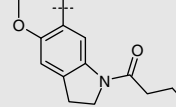
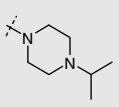
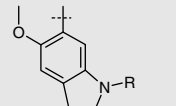
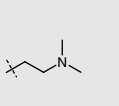
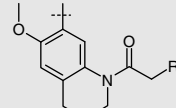
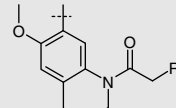
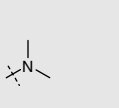
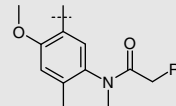
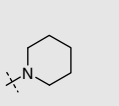
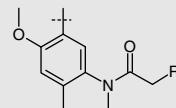
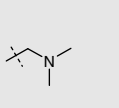
**Scheme 1.** Reagents and conditions: (a)  $\text{Ac}_2\text{O}$ ,  $\text{HNO}_3$ , 65%; (b)  $\text{HCl}$ ,  $\text{MeOH}$ , reflux, 94%; (c)  $\text{BrCH}_2\text{COCl}$ ,  $\text{K}_2\text{CO}_3$ ,  $\text{THF}$  or acryloyl chloride,  $\text{Et}_3\text{N}$ ,  $\text{THF}$ , then amine, 40–90%; (d)  $\text{Pd/C}$ ,  $\text{H}_2$ , 65–95%; (e)  $\text{NaNO}_2$ ,  $\text{TFA}$ ; 70%; (f)  $\text{BH}_3\text{-DMS}$ ,  $\text{THF}$ , 70%.

**Table 3**

IGF-1R enzyme/Delfia, JNK1 results for **20–39** (values represent an average of  $\geq 2$  individual measurements)

Compound	R	IGF-1R enzyme $\text{IC}_{50}$ (nM)	Phospho IGF-1R cellular $\text{IC}_{50}$ (nM)	JNK1 enzyme $\text{IC}_{50}$ (nM)
<b>20</b>		6	278	126
<b>21</b>		4	765	1000
<b>22</b>		2	79	1995
<b>23</b>		1	56	1585
<b>24</b>		3	19	3162
<b>25</b>		50	877	794
<b>26</b>		2	85	1000
<b>27</b>		1	24	1259
<b>28</b>		1	128	1995
<b>29</b>		32	7762	631
<b>30</b>		13	72	126

Table 3 (continued)

Compound		R	IGF-1R enzyme IC <sub>50</sub> (nM)	Phospho IGF-1R cellular IC <sub>50</sub> (nM)	JNK1 enzyme IC <sub>50</sub> (nM)
31			32	376	1585
32			8	191	794
33			6	298	251
34			4	651	1585
35			40	794	100
36		H	25	1984	7943
37			1	16	6310
38			1	11	2512
39			10	209	7943

Compounds **40** and **23** are closely related analogs differing by only a single methyl on the C2'' carboxamide at the C4 aniline.<sup>16</sup> Moreover, like **23**, **40** is a potent IGF-1R inhibitor (enzyme IC<sub>50</sub> = 2 nM, phospho IGF-1R cellular IC<sub>50</sub> = 85 nM) which is also selective for this kinase over JNK1/3 (enzyme IC<sub>50</sub> = 5010/2000 nM).<sup>17</sup> Given the high sequence identity (~80%) between IGF-1R and IR in the kinase domain, we reasoned that the binding mode of **40** in IGF-1R would be nearly identical to that observed in IR. The crystal structure showed that **40** formed two favorable interactions with Asp1083 (Fig. 2). One is an H-bond interaction of the amide carbonyl with the residue's backbone NH; the second is an ionic interaction with the side chain carboxylate. Asp1083 in the IR mutant

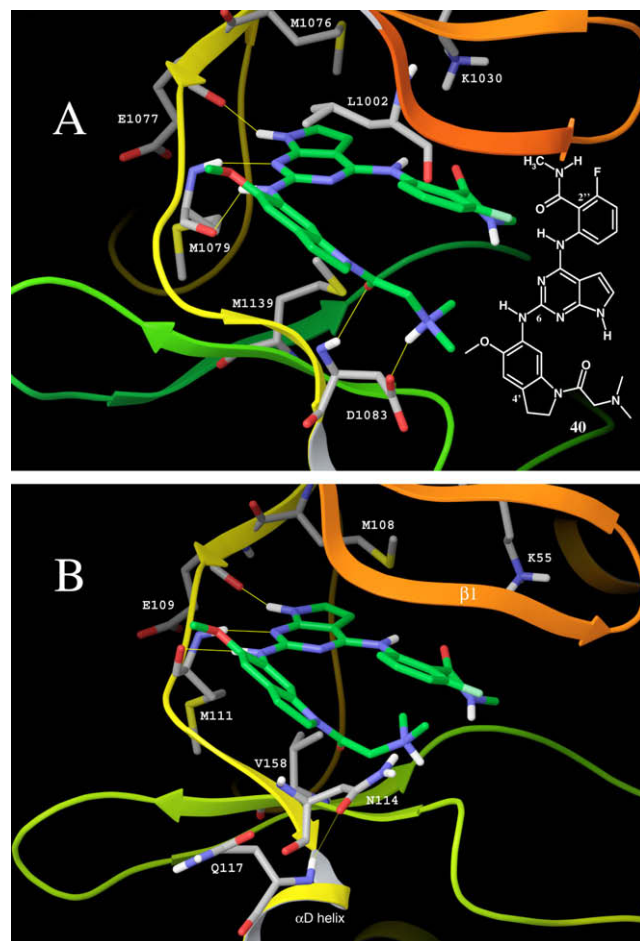


Figure 2. (A) Co-crystal structure of IR Double Mutant (C981S, D1132N, carbon atoms in gray) in complex with **40** (carbon atoms in green). Intermolecular H-bond interactions are highlighted with yellow lines. (B) Structural model of JNK1 (carbon atoms in gray) in complex with **40**. Intermolecular H-bond and ionic interactions are highlighted with yellow lines.

Table 4

*In vivo* rat DMPK Properties for selected analogs (values represent the average of three animals)

Compound	Dose (mg/kg)		CL (mL/min/kg)	po DNAUC (0–8 h) (ng h/mL/mg/kg)	po C <sub>max</sub> (ng/mL)	% F
	iv	po				
<b>2</b>	—	9.0	—	133	233	—
<b>4</b>	2.5	13.0	112	85	192	60
<b>23</b>	2.6	13.0	48	190	455	61
<b>40</b>	2.5	10.0	73	210	365	98

corresponded to Asp1056 in IGF-1R which formed an ionic interaction with the ionizable isopropyl amine in **2** (see structural model in Fig. 1). This interaction of the *N,N*-dimethyl glycine side chain with the aspartate residue may explain why the carbonyl group, its distance from the ionizable amine, and the nature of the amine are important in maintaining a certain degree of activity against IGF-1R. Modeling efforts were initiated to understand the selectivity against JNK1 and 3. To that end a sequence alignment of IGF-1R, IR, JNK1, and JNK3 was generated, which was then used to superimpose X-ray structures of all four protein kinases, and a plausible explanation was identified. If we assume a similar binding mode for **40** in JNK1 and 3,<sup>18</sup> we first observed that an asparagine (Asn114 in JNK1, Asn152 in JNK3) corresponded to the

Asp1056 of IGF-1R (or Asp1083 for IR). We recognized that the asparagine's side chain carbonyl could form an H-bond with the inhibitor's protonated amine. However, as revealed by numerous JNK X-ray structures, we found in our structural model (Fig. 2B) that the carbonyl instead formed an internal H-bond interaction with the enzyme's backbone. In all cases, the amino group of the asparagine was directed up towards the  $\beta$ 1 strand, which would place it in proximity to the inhibitor's protonated amine, potentially producing a non-favorable interaction. Thus the placement of ionizable amines in the vicinity of the Asn leads to the observed selectivity.

The in vivo rat pharmacokinetic properties of selected analogs are listed in Table 4. While the lead piperazine **2** and the unconstrained analog **4** had reasonable oral exposure, the in vivo clearance for **4** was quite high. Gratifyingly the indoline analogs **23** and **40** demonstrated better exposure (DNAUC) and higher maximum concentrations ( $C_{\max}$ ) after oral administration. The excellent oral bioavailability of **40**, coupled with its potency and selectivity profile, makes it a preferred candidate for advanced in vivo pharmacodynamic studies.<sup>15,16</sup>

In summary, detailed investigation of C5' substituents of 4,6-bis-anilino-1H-pyrrolo[2,3-d]pyrimidines revealed a set of compounds with nanomolar inhibition of the IGF-1R tyrosine kinase in enzymatic and cellular assays. An unprecedented interaction of ionizable terminal amines at C5', sensitive to conformational flexibility, with aspartate residue 1056 in IGF-1R was discovered. The amide carbonyl of the *N,N*-dimethyl glycine analogs participated in an additional H-bond with the backbone NH of the aspartate residue. These basic amine containing functional groups also imparted a 1000-fold selectivity over JNK which was not attained by previously reported C4' substituted analogs. Molecular modeling shed light on a possible explanation for this selectivity. The examination of rodent pharmacokinetics of selected analogs provided promising compounds, especially **23** and **40**, which could be used orally for biological characterization.

## Acknowledgments

The authors thank Julie Mosley, Giorgia Vicentini, and Emma Jones for the crystal structure in the supporting information.<sup>18</sup>

## Supplementary data

Supplementary data associated with this article can be found, in the online version, at doi:10.1016/j.bmcl.2008.11.077.

## References and notes

- For recent reviews see: (a) Hartog, H.; Wesseling, J.; Boezen, H. M.; van der Graaf, W. T. A. *Eur. J. Cancer* **2007**, *43*, 1895; (b) Casa, A. J.; Dearth, R. K.; Litzzenburger, B. C.; Lee, A. V.; Cui, X. *Front. Biosci.* **2008**, *13*, 3906.
- (a) Rodon, J.; DeSantos, V.; Ferry, R. J., Jr.; Kurzrork, R. *Mol. Cancer Ther.* **2008**, *7*, 2575; (b) Sarma, P. K. S.; Tandon, R.; Gupta, P.; Dastidar, S. G.; Ray, A.; Das, B.; Cliffe, I. A. *Expert Opin. Ther. Patents* **2007**, *17*, 25.
- Chamberlain, S. D.; Atkins, C.; Deanda, F.; Groy, A.; Kumar, R.; Leesnitzer, M. A.; Lei, H.; Moorthy, G.; Patnaik, S.; Quinn, R.; Redman, A. M.; Rowland, J.; Sabbatini, P.; Shewchuck, L.; Stevens, K. L.; Wilson, J. W.; Yang, B.; Shotwell, J. B. *Bioorg. Med. Chem. Lett.* Preceding communication.
- The IGF-1R enzyme and cellular assays have been described in the reference section of the preceding communication: Chamberlain, S. D.; Atkins, C.; Deanda, F.; Groy, A.; Kumar, R.; Leesnitzer, M. A.; Lei, H.; Moorthy, G.; Patnaik, S.; Quinn, R.; Redman, A. M.; Rowland, J.; Sabbatini, P.; Shewchuck, L.; Stevens, K. L.; Wilson, J. W.; Yang, B.; Shotwell, J. B. *Bioorg. Med. Chem. Lett.* Preceding communication.
- Description of the JNK1/3 enzyme assay protocols are provided in the supplementary data section.
- Davis, R. J. *Cell* **2000**, *103*, 239.
- (a) Bogoyevitch, M. A.; Kobe, B. *Microbiol. Mol. Biol. Rev.* **2006**, *70*, 1061; (b) Barr, R. K.; Bogoyevitch, M. A. *Int. J. Biochem. Cell Biol.* **2001**, *33*, 1047.
- Nateri, A. S.; Spencer-Dene, B.; Behrens, A. *Nature* **2005**, *437*, 281.
- Kracht, M. *Anti-Inflamm. Anti-Allergy Agents Med. Chem.* **2007**, *6*, 71.
- A description of the interactions of **1** with the kinase domain of IGF-1R and IR has been presented in the preceding communication.
- Trends in the data for JNK3 were very similar to that of JNK1. Only the JNK1 data is reported in Tables 2 and 3 for brevity.
- Chamberlain, S.; Lei, H.; Patnaik, S.; Gerding, R.; Redman, A.; Stevens, K.; Wilson, J.; Yang, B.; Shotwell, J.; Moorthy, G. *J. Org. Chem.* **2008**, *73*, 9511.
- Iyobe, A.; Uchida, M.; Kamata, K.; Hotei, Y.; Kusama, H.; Harada, H. *Chem. Pharm. Bull.* **2001**, *49*, 822.
- IR protein was expressed and purified as previously described in Li, S.; Covino, N. D.; Stein, E. G.; Till, J. H.; Hubbard, S. R. *J. Biol. Chem.* **2003**, *278*, 26007. Protein at 10 mg/mL was complexed with a 3-fold molar excess of inhibitor for 1 h prior to crystallization. Crystals were grown by hanging drop vapor diffusion at 22 °C from 0.1 M MOPS, pH 7.0, 1.0 M trisodium citrate. Crystals were flash frozen in PFO prior to data collection. The structure was solved by molecular replacement using PDB/1P14 as a starting model and refined to an *R*-factor of 20% at 2.1 Å using REFMAC. Crystallographic data for the structure A in Figure 2 have been deposited at PDB/3EKK.
- The insulin receptor (IR) enzyme and phospho IR cellular IC<sub>50</sub> values for **40** were 1.8 nM and 79 nM, respectively. The pyrrolopyrimidines described in this communication were, to all intents and purposes, equipotent against IR. The toxicity implications of not having selectivity toward IR have been addressed with respect to compound **40** in an account that has been recently submitted to *Cancer Research*. The article includes the measurement of metabolic endpoints after oral administration of various doses of **40** in mice.
- With similarly substituted C6 anilines the *N*-methyl C2'' carboxamides displayed the same SAR trends as the unsubstituted C2'' carboxamides listed in Tables 2 and 3.
- Estimates of the impact of plasma protein binding on overall potency for **23** and **40** could be made by carrying out the phospho IGF-1R cellular assay (see reference section in preceding communication) in the presence of 2% HSA and 0.1% AAG. Under these conditions, the observed IC<sub>50</sub> values for **23** and **40** were 487 and 310 nM, respectively.
- There is a crystal structure of a 4,6-bis-anilino-1H-pyrrolo[2,3-d]pyrimidine derivative in complex with JNK1 (PDB/3ELJ) which is consistent with the structural model in Figure 2, B. Please see supplementary data.